

Extreme vortex pinning in the noncentrosymmetric superconductor CePt₃Si

C. F. Miclea*

Max-Planck-Institute for Chemical Physics of Solids, 01187 Dresden, Germany and National Institute for Materials Physics, 077125 Bucharest-Magurele, Romania

A. C. Mota

Max-Planck-Institute for Chemical Physics of Solids, 01187 Dresden, Germany and Solid State Laboratory, ETH Zurich, CH-8093 Zurich, Switzerland

M. Nicklas, R. Cardoso, and F. Steglich

Max-Planck-Institute for Chemical Physics of Solids, 01187 Dresden, Germany

M. Sigrist

Institute for Theoretical Physics, ETH Zurich, CH-8093 Zurich, Switzerland

A. Prokofiev and E. Bauer

Institut für Festkörperphysik, Technische Universität Wien, A-1040 Wien, Austria

(Received 9 December 2009; published 28 January 2010)

We report on the vortex dynamics of a single crystal of the noncentrosymmetric heavy-fermion superconductor CePt₃Si. Decays of the remnant magnetization display a logarithmic time dependence with rates that follow the temperature dependence expected from the Kim-Anderson theory. The creep rates are lower than observed in any other centrosymmetric superconductor and are not caused by high critical currents. On the contrary, the critical current in CePt₃Si is considerably lower than in other superconductors with strong vortex pinning indicating that an alternative impediment on the flux-line motion might be at work in this superconductor.

DOI: [10.1103/PhysRevB.81.014527](https://doi.org/10.1103/PhysRevB.81.014527)

PACS number(s): 74.25.Uv, 71.27.+a, 74.25.Bt

I. INTRODUCTION

Unconventional superconductors which violate spontaneously other symmetries beside the $U(1)$ -gauge symmetry have been found to show many intriguing properties. Among such superconductors Sr₂RuO₄, PrOs₄Sb₁₂, and possibly UPt₃ have been identified as time-reversal symmetry breaking by means of zero-field μ SR studies.¹ These compounds show surprisingly slow vortex dynamics with creep rates lower than in any other superconductor.²⁻⁴ It has been proposed that this behavior is connected with the presence of domain walls between different degenerate superconducting phases which would occur naturally in time-reversal symmetry-breaking states. Such domain walls could act as barriers for vortices, rather than the pinning of vortices at impurities and defects.⁵ The latter pinning mechanism would have implied very high critical currents unlike what was observed in the experiments.

Our investigation of the heavy-fermion superconductor CePt₃Si (Ref. 6) reveals extremely slow flux dynamics with creep rates even lower than those in Sr₂RuO₄,² PrOs₄Sb₁₂,³ and UPt₃.⁴ Interestingly, the critical current in CePt₃Si is also low, in spite of the fact that this superconductor does not break time-reversal symmetry. CePt₃Si is a member of a whole class of presumably unconventional heavy-fermion superconductors such as CeRhSi₃,⁷ CeIrSi₃,⁸ and UIr (Ref. 9) whose crystal lattices do not possess an inversion center. Among these noncentrosymmetric compounds, CePt₃Si is the only one where superconductivity sets in already at ambient pressure. Unconventional features in the superconduct-

ing properties of systems without inversion symmetry has been discovered also outside the heavy-fermion class as, for example, in Li₂(Pd,Pt)₃B (Refs. 10 and 11) or Mg₁₀Ir₁₉B₁₆.¹²

In CePt₃Si antiferromagnetic order sets in at a Néel temperature $T_N=2.2$ K while the system adopts a superconducting ground state below a transition temperature $T_c=0.75$ K for polycrystalline samples.⁶ Lower superconducting transition temperatures have been reported for single crystals.¹³ Long-range magnetic order coexists with superconductivity on a microscopic scale as revealed by μ SR investigations.¹⁴ The upper critical field $H_{c2}\approx 3-5$ T exceeds the Pauli-Clogston limit $H_p\approx 1.1$ T indicating that paramagnetic depairing is unimportant here. Knight-shift data actually display no reduction in the spin susceptibility below T_c , for magnetic fields perpendicular or parallel to the crystallographic c axis.¹⁵ Power laws describing the low-temperature behavior of thermal conductivity,¹⁶ penetration depth,¹⁷ $1/T_1$ relaxation rate,¹⁸ and specific heat¹³ observed in CePt₃Si suggests a superconducting gap with line nodes. Remarkably, CePt₃Si is the only heavy-fermion system to exhibit a Hebel-Slichter coherence peak below T_c ,¹⁸ a feature characteristic to an s -wave superconductor. The main part of this work is an experimental investigation of flux dynamics on a single crystal of CePt₃Si which reveals the presence of an unconventional and very effective vortex-pinning mechanism.

II. CHARACTERIZATION OF THE SAMPLE AND THE SUPERCONDUCTING PHASE

The high-quality CePt₃Si single crystal investigated was grown using a Bridgman technique and the sample was ori-

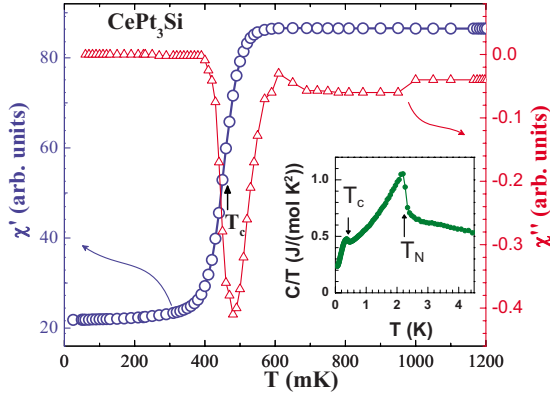


FIG. 1. (Color online) Temperature dependences of the real the imaginary part of the ac magnetic susceptibility across the superconducting phase transition. Inset: temperature dependence of the specific heat divided by temperature.

ented, cut, and polished in a parallelepiped shape with the dimensions $4.60 \text{ mm} \times 2.65 \text{ mm} \times 1.05 \text{ mm}$. The longer dimension is parallel to the crystallographic a axis while the smaller one is parallel to the b axis. An investigation of the single crystal for twinning (two distinct noncentrosymmetric atomic configurations) was performed by a new refinement of the crystal structure of CePt_3Si from x-ray intensity data. It shows a contribution of 87% of the main inversion twin component.

Prior to the flux creep measurements the sample was characterized by ac magnetic susceptibility and specific heat. The investigation of vortex dynamics was performed in a dilution refrigerator in the temperature range $0.1 \leq T \leq 0.5 \text{ K}$ with the sample enclosed in a custom-built mixing chamber and using a superconducting quantum interference device (SQUID) detector to determine the magnetic flux expelled. The external magnetic field applied to drive the sample into the Bean critical state was applied along the a axis. In the same experimental configuration, ac susceptibility experiments were performed in the temperature range $0.025 \leq T \leq 2.4 \text{ K}$ using an inductance bridge with a SQUID as null detector. A very low ac excitation field of $H = 1.3 \text{ mOe}$ was applied along the a axis at a frequency $f = 80 \text{ Hz}$. The temperature dependence of the specific heat was measured in the temperature range $0.05 \leq T \leq 4.5 \text{ K}$ employing a quasiadiabatic pulse method.

Both, the real, χ' , and the imaginary, χ'' , part of the ac susceptibility (Fig. 1) clearly reveal the superconducting transition with the midpoint of the anomaly in χ' located at $T_c = 0.45 \text{ K}$, a value much lower than the one obtained for polycrystals. The transition width, defined as the temperature difference between the 10% and 90% drop of the real part of susceptibility across the anomaly, is $\Delta T = 0.1 \text{ K}$ also substantially smaller than the value observed for polycrystalline samples. Moreover, our finding is in excellent agreement with previous studies on high-quality single crystals.¹³ The T_c discrepancy between single crystal and polycrystal is not yet properly understood, but one possible explanation is that this compound has an homogeneity range¹⁹ similar, for example, to the well-known case of CeCu_2Si_2 ,²⁰ which allows for homogeneous samples with slightly different composi-

tions but substantially different physical properties to form. Another scenario²¹ suggests that twin boundaries could enhance the trend to superconductivity in polycrystalline samples. Upon warming up the sample in the normal state, χ' and χ'' become temperature independent up to $T = 2.4 \text{ K}$ and no signature of the transition from the long-range magnetically ordered state into the paramagnetic phase was detected, for our field orientation ($H \parallel a$).

The temperature dependence of the specific heat divided by temperature is depicted in the inset of Fig. 1. The transition into the antiferromagnetically ordered state is clearly visible as a sharp peak at $T_N = 2.3 \text{ K}$, a value consistent with the one obtained in previous specific-heat studies.¹³ Upon further cooling down, the system adopts a superconducting ground state at $T_c = 0.42 \text{ K}$, in good agreement with our susceptibility data and Ref. 13. Both T_N and T_c are defined as the midpoint of the jump in C across the respective anomaly. The C/T data in the temperature range $0.5 \leq T \leq 2.1 \text{ K}$ are well described by $C/T = 423 \text{ mJ}/(\text{mol K}^2) + 140T^2 \text{ mJ}/(\text{mol K}^4)$. We remove the phononic and antiferromagnetic contributions to the specific heat by subtracting $140T^3 \text{ mJ}/(\text{mol K}^4)$ from the $C(T)$ data and obtain a normal-state Sommerfeld coefficient $\gamma_n = 400 \text{ mJ}/(\text{mol K}^2)$. This leads to a jump of the specific heat at the superconducting phase transition of $\Delta C/(\gamma_n T_c) \approx 0.29$, a value situated significantly below the BCS-theory prediction of $\Delta C/(\gamma_n T_c) = 1.43$. In the superconducting state, C exhibits a quadratic temperature dependence down to $T = 0.1 \text{ K}$ rather than an exponential one, indicative of the existence of line nodes in the superconducting gap.²² A zero-temperature interception of the quadratic specific heat would yield a residual electronic specific-heat coefficient with a finite value of $\gamma_s = 145 \text{ mJ}/\text{mol K}^2$. However, below $T = 0.1 \text{ K}$, the specific heat has a weaker temperature dependence, therefore the residual γ_s will assume probably an even higher value and partially account for the very low value of $\Delta C/(\gamma_n T_c)$.

III. FLUX DYNAMICS MEASUREMENTS

Isothermal relaxation curves of the remnant magnetization M_{rem} were taken after cycling the specimen in an external dc magnetic field H applied along the crystallographic a direction. Vortices were introduced into the sample at a constant and slow rate in order to avoid eddy-current heating and using, at the lowest temperature, a magnetic field just high enough to drive the sample into the Bean critical state. The required magnetic field was kept constant in the sample for several minutes and then gradually reduced to zero. Immediately after, the relaxation of the metastable magnetization was recorded with a digital flux counter for several hours. The time required to ramp down the field is negligible compared with the time of the relaxation measurement. At the lowest temperature of our investigation, $T = 100 \text{ mK}$, we determined the field corresponding to the Bean critical state, H^* , by estimating the field H_s where the remnant magnetization saturates as a function of the applied external magnetic field ($H_s \approx 2H^*$). For this sample, we found $H_s = 500 \text{ Oe}$ at $T = 100 \text{ mK}$ (inset of Fig. 2). At higher temperatures the sample is in the critical state already for smaller external

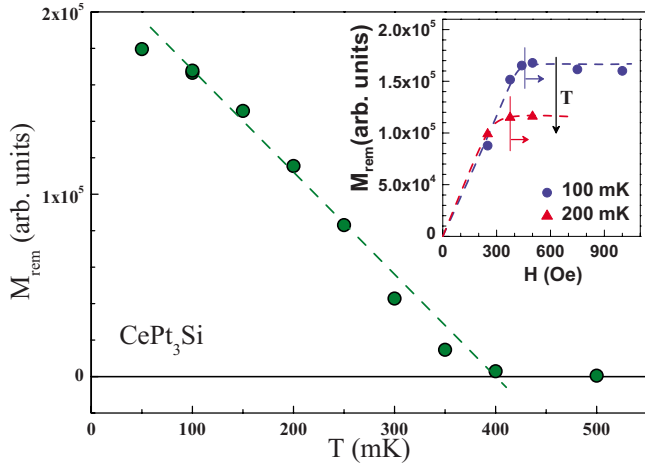


FIG. 2. (Color online) Temperature dependence of the total remnant magnetization. Dashed line is a linear fit to the data. Inset: total remnant magnetization at $T=0.1$ K and $T=0.2$ K as function of the external magnetic field H .

fields since H_s decreases upon increasing T as demonstrated in the inset of Fig. 2. In the main part of Fig. 2, we present the temperature dependence of the remnant magnetization obtained after cycling the sample in a field of $H=500$ Oe. To obtain the value of M_{rem} , after removing the field at constant temperature we warmed up the sample well above T_c and recorded the total magnetic flux expelled. M_{rem} decreases monotonically upon increasing temperature with the experimental data well described by a linear fit (dashed line in Fig. 2) which intercepts zero at around $T \approx 0.41$ K. This is in excellent agreement with the value of T_c yielded by ac susceptibility and specific-heat measurements. In light of the comparison between the single-crystalline and polycrystalline $CePt_3Si$ samples, it is important to remark that at $T=0.5$ K no flux was trapped in the crystal clearly showing that the bulk of the sample is well in the normal state at this temperature.

Isothermal decays of the remnant magnetization at different temperatures are depicted in Fig. 3. At constant temperature the flux escaping the sample is recorded typically for more than 10^4 s. Then the sample is heated up above T_c so all the trapped field is expelled out of the sample (inset of Fig. 3). In this way we obtain the value of the total remnant magnetization as the sum of the amount of flux expelled in the first 10^4 s plus the flux removed while crossing T_c . This value of M_{rem} is then used to normalize the creep rate. At all temperatures the decays show a logarithmic time dependence as predicted by the Kim-Anderson theory.²³ The creep rate becomes faster upon increasing the temperature as expected for thermally activated flux motion. The temperature dependence of the normalized relaxation rates $S = \partial \ln(M) / \partial \ln(t)$ for $CePt_3Si$ is depicted in Fig. 4 together with the rates obtained for the heavy-fermion superconductor UBe_{13} (Refs. 3 and 4) which only breaks gauge symmetry, $PrOs_4Sb_{12}$ (Ref. 3) which, in addition, violates time-reversal symmetry and the noncentrosymmetric superconductor Li_2Pt_3B .²⁴ Remarkably, $CePt_3Si$ has anomalously small decay rates comparable only with Li_2Pt_3B and lower by a factor of five than the very low creep rates observed in $PrOs_4Sb_{12}$. Li_2Pt_3B breaks the

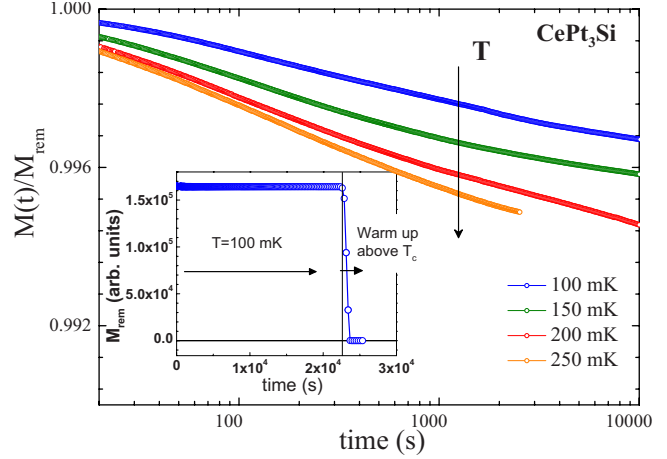


FIG. 3. (Color online) Normalized remnant magnetization as a function of time at different constant temperatures. Inset: remnant magnetization as a function of time at $T=0.1$ K. After 2.25×10^4 s the sample is warmed up above T_c and all the trapped magnetic flux is expelled.

inversion symmetry and displays extremely small creep rates as well. However, for the latter compound, in a certain temperature interval, the weak initial logarithmic creep is followed after several thousand seconds by a much faster, avalanche-like, also logarithmic, decay.²⁴

In general in superconductors with strong vortex pinning the critical current j_c is high. However, this is not the case in $CePt_3Si$ which has the lowest critical current [$j_c(300$ mK) = 1.8×10^7 A/m²] among the compared superconductors (Fig. 5). As the temperature is the relevant parameter in the thermally activated motion of vortices it is important to com-

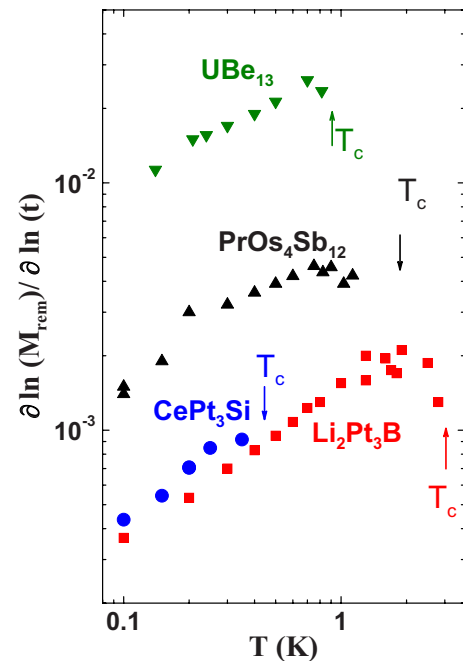


FIG. 4. (Color online) Comparison of the normalized relaxation rates $S = \partial \ln(M) / \partial \ln(t)$ as function of temperature for different compounds in a log-log representation.

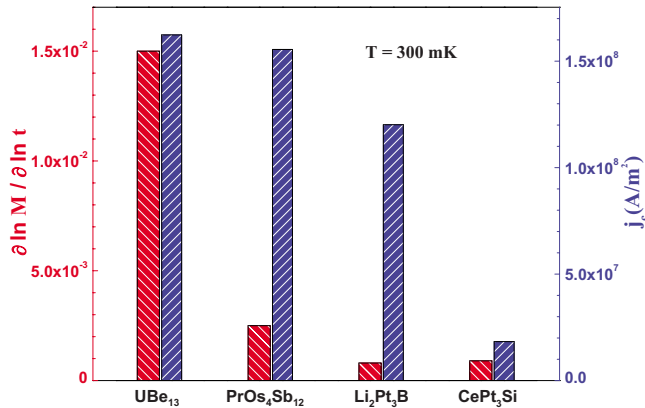


FIG. 5. (Color online) Comparison of the normalized relaxation rates $S = \partial \ln(M) / \partial \ln(t)$ and the critical current at $T = 0.3$ K for different compounds. For each compound the left bar depicts S and the right one j_c .

pare the relaxation rates of the different compounds at the same temperature. The comparison depicted in Fig. 5 has been done for $T = 300$ mK and in the framework of the Bean model which assumes a constant $j_c(T) \propto H^*(T)/d$, where d is the thickness of the platelike-shaped sample. In Fig. 5 we also plot the critical currents at the same temperature as the relaxation rates in order to understand their relevance for the pinning process. If we compare the critical currents j_c of the two noncentrosymmetric compounds at $T = 300$ mK we find $j_c(\text{Li}_2\text{Pt}_3\text{B})/j_c(\text{CePt}_3\text{Si}) \approx 7$. Even at the same T/T_c the critical current in CePt₃Si is more than 40% lower in comparison with Li₂Pt₃B. Therefore, one conclusion deduced from Fig. 5 is that the critical current is not the relevant parameter for the pinning mechanism in CePt₃Si. A lower critical current for CePt₃Si is reflected in a reduced vortex density which could explain the lack of avalanchelike relaxation.

The extremely slow vortex dynamics in CePt₃Si in combination with the comparatively small critical current suggests that an unconventional and very effective pinning mechanism is at work. Similar effects had been seen in UPt₃, Sr₂RuO₄, and PrOs₄Sb₁₂ and have been associated with an intrinsic pinning mechanism on domain walls existing due to time-reversal symmetry violation in these superconductors.⁵

However, CePt₃Si does not break time-reversal symmetry. It has been recently proposed by Iniotakis *et al.*²¹ that twin boundaries in twinned crystals could play a similar role in noncentrosymmetric superconductors and yield a very strong flux-line pinning due to the fractionalization of vortices. So twin boundaries could act as planar barriers for flux flow without affecting the critical current. While this could be an explanation for the observed behavior in CePt₃Si and also provides a possible mechanism for the flux avalanches reported for Li₂Pt₃B,²⁴ there has been no direct observation of such flux-line pinning on twin boundaries so far.

IV. CONCLUSION

In conclusion, we observed extremely slow vortex dynamics in the noncentrosymmetric CePt₃Si in spite of a very low critical current. The relaxation rates are comparable only to the similarly noncentrosymmetric Li₂Pt₃B which has as well a modest critical current though larger than in CePt₃Si. This apparent contradiction of extremely low relaxation rates in conjunction with low critical currents indicates an unconventional and very effective flux trapping mechanism. A possible explanation of this pinning mechanism could be the existence of fractionalized vortices localized on the twin boundaries of the noncentrosymmetric crystal. However, this scenario needs independent verification apart from the flux dynamics reported here. No other explanations of the observed phenomena are known to us to date. Unlike in Li₂Pt₃B we did not observe flux avalanches.²⁴ This might be due to the much lower flux density reflected by the reduced critical current in CePt₃Si.

ACKNOWLEDGMENTS

We are grateful to the late Kazumi Maki for many enlightening and useful discussions on this subject. C.F.M would like to acknowledge the support of the German Research Foundation (DFG) under the auspices of the MI 1171/1-1. A.C.M. and M.S. have been financially supported by the Swiss Nationalfonds and the NCCR MaNEP. E.B. is grateful to the Austrian FWF P18054.

*miclea@cpfs.mpg.de

¹Y. Aoki, T. Tayama, T. Sakakibara, K. Kuwahara, K. Iwasa, M. Kohgi, W. Higemoto, D. E. Maclaughlin, H. Sugawara, and H. Sato, *J. Phys. Soc. Jpn.* **76**, 051006 (2007).

²E. M. M. Dumont, Ph.D. thesis, ETH, 2000.

³T. Cichorek *et al.* (unpublished).

⁴A. Amann, A. C. Mota, M. B. Maple, and H. von Löhneysen, *Phys. Rev. B* **57**, 3640 (1998).

⁵M. Sigrist and D. Agterberg, *Prog. Theor. Phys.* **102**, 965 (1999).

⁶E. Bauer, G. Hilscher, H. Michor, Ch. Paul, E. W. Scheidt, A. Griбанov, Yu. Seropegin, H. Noel, M. Sigrist, and P. Rogl, *Phys. Rev. Lett.* **92**, 027003 (2004).

⁷N. Kimura, K. Ito, K. Saitoh, Y. Umeda, H. Aoki, and T.

Terashima, *Phys. Rev. Lett.* **95**, 247004 (2005).

⁸I. Sugitani, Y. Okuda, H. Shishido, T. Yamada, A. Thamizhavel, E. Yamamoto, T. D. Matsuda, Y. Haga, T. Takeuchi, R. Settai, and Y. Onuki, *J. Phys. Soc. Jpn.* **75**, 043703 (2006).

⁹T. Akazawa, H. Hidaka, T. Fujiwara, T. C. Kobayashi, E. Yamamoto, Y. Haga, R. Settai, and Y. Onuki, *J. Phys.: Condens. Matter* **16**, L29 (2004).

¹⁰K. Togano, P. Badica, Y. Nakamori, S. Orimo, H. Takeya, and K. Hirata, *Phys. Rev. Lett.* **93**, 247004 (2004).

¹¹P. Badica, T. Kondo, and K. Togano, *J. Phys. Soc. Jpn.* **74**, 1014 (2005).

¹²T. Klimczuk, Q. Xu, E. Morosan, J. D. Thompson, H. W. Zandbergen, and R. J. Cava, *Phys. Rev. B* **74**, 220502(R) (2006).

- ¹³T. Takeuchi, M. Tsujin, T. Yasuda, S. Hashimoto, R. Settai, and Y. Onuki, *J. Magn. Magn. Mater.* **310**, 557 (2007).
- ¹⁴A. Amato, E. Bauer, and C. Baines, *Phys. Rev. B* **71**, 092501 (2005).
- ¹⁵M. Yogi, H. Mukuda, Y. Kitaoka, S. Hashimoto, T. Yasuda, R. Settai, T. D. Matsuda, Y. Haga, Y. Onuki, P. Rogl, and E. Bauer, *J. Phys. Soc. Jpn.* **75**, 013709 (2006).
- ¹⁶K. Izawa, Y. Kasahara, Y. Matsuda, K. Behnia, T. Yasuda, R. Settai, and Y. Onuki, *Phys. Rev. Lett.* **94**, 197002 (2005).
- ¹⁷I. Bonalde, W. Brämer-Escamilla, and E. Bauer, *Phys. Rev. Lett.* **94**, 207002 (2005).
- ¹⁸M. Yogi, Y. Kitaoka, S. Hashimoto, T. Yasuda, R. Settai, T. D. Matsuda, Y. Haga, Y. Onuki, P. Rogl, and E. Bauer, *Phys. Rev. Lett.* **93**, 027003 (2004).
- ¹⁹A. V. Gribanov, Y. D. Seropegin, A. I. Tursina, O. I. Bodak, P. Rogl, and H. Noel, *J. Alloys Compd.* **383**, 286 (2004).
- ²⁰F. Steglich, P. Gegenwart, C. Geibel, R. Helfrich, P. Hellmann, M. Lang, A. Link, R. Modler, G. Sparn, N. Büttgen, and A. Loidl, *Physica B* **223-224**, 1 (1996).
- ²¹C. Iniotakis, S. Fujimoto, and M. Sigrist, *J. Phys. Soc. Jpn.* **77**, 083701 (2008).
- ²²K. V. Samokhin, E. S. Zijlstra, and S. K. Bose, *Phys. Rev. B* **69**, 094514 (2004).
- ²³P. W. Anderson and Y. B. Kim, *Rev. Mod. Phys.* **36**, 39 (1964).
- ²⁴C. F. Miclea, A. C. Mota, M. Sigrist, F. Steglich, T. A. Sayles, B. J. Taylor, C. A. McElroy, and M. B. Maple, *Phys. Rev. B* **80**, 132502 (2009).